Ab initio studies of sperrylite, platarsite and palladoarsenide bulk and surface stabilities

B Nemutudi, P P Mkhonto and P E Ngoepe

Materials Modelling Centre, University of Limpopo, Private Bag x1106, Sovenga 0727, South Africa

Email: bradley.nemutudi@ul.ac.za

Abstract. In this study we employed the Vienna *Ab-initio* Simulation Package (VASP) along with the projector augmented wave (PAW) pseudopotential method to investigate the bulk structural and surface stabilities of sperrylite ($PtAs_2$), platarsite (PtAsS) and palladoarsenide (Pd_2As) minerals. The phase stability of PtAsS was obtained using cluster expansion. The phonon dispersion curves showed no soft modes for all the structures, suggesting stability. The calculated surface energies indicated that the (100) surface was the most stable amongst the low Miller index (100), (110) and (111) surfaces for $PtAs_2$, PtAsS and Pd_2As. The order of surface energies increased as: (100) < (111) < (110) for $PtAs_2$ and PtAsS and (100) < (110) < (111) for Pd_2As. The calculated thermodynamically equilibrium morphologies of the relaxed surface structures indicated that the (100) surface was the most dominant for all the studied structures. The findings offer more insight on the stability of these minerals which may be applicable in their recovery.

1. Introduction

South Africa is one of the leading countries with high percentage of platinum group metal (PGM) in the igneous intrusion of Platreef Bushveld Complex [1]. The most predominant PGMs are platinum (Pt) and palladium (Pd) which consist of about 21% of arsenides [2]. Platinum is extremely resistant to physical and chemical degradation and has exceptional catalytic properties. These properties have led to extensive utilization of jewelry, high temperature industrial and automobile markets [3]. The stability of $PtAs_2$, PtAsS and Pd_2As is important in understanding their mineralogy formation and therefore to their recovery. Furthermore, PGMs which contain both sulphur and arsenide are complex and need a detailed understanding of their stability. First principle calculations have become an important tool for surface scientists as they can determine facet-specific surface energies, surface electronic structures and crystal morphologies [4].

In this paper, we performed density functional theory (DFT) calculations to study structural and vibrational stability of $PtAs_2$, PtAsS and Pd_2As models. The cluster expansion was implemented to generate the platarsite (PtAsS) mix bulk model. The surface calculations were computed to identify the most stable surface (working surface) for $PtAs_2$, PtAsS and Pd_2As minerals. These were complemented with surface morphology in order to identify the preferred plane cleavages.

2. Computational methodology

The bulk and surface stability calculations were performed within the framework of *ab-initio* quantum mechanical density functional theory [5]. The plane-wave (PW) projector augmented wave

pseudopotential with the generalized gradient approximation of Perdew-Burke-Ernzerhof (GGA-PBE) exchange-correlation [6], implemented within the VASP code [7], were employed. The plane-wave cut-off energy was set to 450 and 500 eV for (PtAs$_2$, PtAsS) and Pd$_2$As bulk models, respectively. The Brillouin zone k-points sampling for bulk model were performed on a grid of $4 \times 4 \times 4$ and $7 \times 7 \times 14$ and for surfaces the $4 \times 4 \times 1$ and $5 \times 3 \times 1$ were used for (PtAs$_2$, PtAsS) and Pd$_2$As. This was chosen according to the scheme proposed by Monkhorst-Pack [8]. The phonon dispersion spectra were computed using the PHONON code [9]. The interaction range of 10.0 Å for phonon dispersion was used for all the models. These were used to investigate the structural and vibrational properties of PtAs$_2$, PtAsS and Pd$_2$As minerals. In addition, cluster expansion within MedeA-UNiversal CLuster Expansion (UNCLE) was performed to generate new stable phase of PtAsS model [10].

To model the surface of the periodic boundary conditions, a slab of finite thickness perpendicular to the surface but infinite extension i.e. using periodic boundary conditions was used. These slabs surfaces were obtained by cleaving the optimized bulk PtAs$_2$, PtAsS and Pd$_2$As structures. Slabs were separated from replicas repeating by a vacuum width of 20 Å. Different terminations were tested and only less reactive (low positive surface energy) for (100), (110) and (111) surfaces were considered.

3. Results and discussion

3.1. Cluster expansion and ground state structures of PtAsS model
In order to minimize the sensitivity of the cluster expansion to the user choices, and to make cluster expansion applicable beyond simple binary systems, a new program package under the name UNiversal CLuster Expansion (UNCLE) [11] has been developed. The UNCLE code [12] predicts the ground states of systems containing up to three and more elements.

For the cluster expansion method we started by searching for the ground state of the PtAsS system of the DFT energy formation. Our initial starting point was PtAs$_2$, where the sulphur atoms were added at the same position as arsenic atoms. The X, Y and Z parameters were also fitted to be equivalent for both As and S atoms.
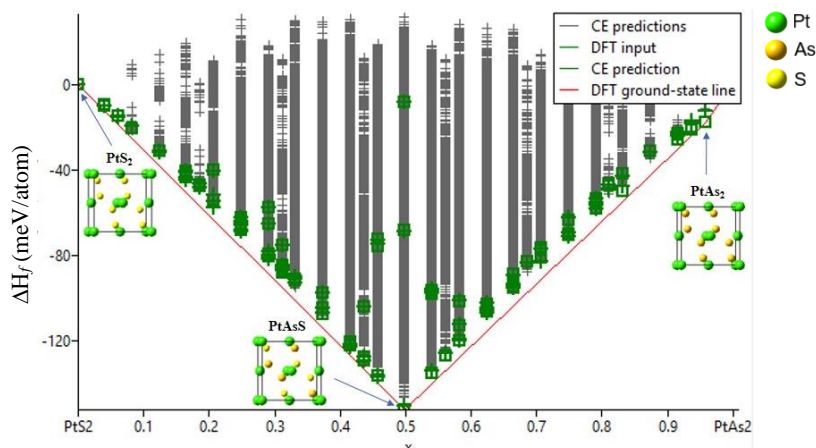

Figure 1: The cluster expansion calculated ground states of Pt-As-S. The energies of formation are with reference to Pt, As and S.

The binary ground state diagram in Figure 1 shows that all generated structures have negative heat of formation (ΔH_f), hence they are thermodynamically stable. Moreover, the cluster expansion showed a greater stability at 50/50 percentage (x = 0.5) where arsenic and sulphur atoms are equal. All structures between PtS$_2$ and PtAs$_2$ i.e. phases of PtAsS are more stable than PtS$_2$ and PtAs$_2$. It is therefore conceivable that a number of phases can form. However, some stoichiometries have multiple DFT inputs. Only three of the stable structures PtS$_2$, PtAsS and PtAs$_2$ are shown in Figure 1.

3.2. Bulk properties of PtAs$_2$, PtAsS and Pd$_2$As

The crystal structures of sperrylite, platarsite are cubic with space group Pa-3 [13] and 12 atoms, while palladoarsenide is monoclinic with space group of P-62m [14] and contain 9 atoms. The PtAs$_2$ and PtAsS supercell structures have 120 atoms, while Pd$_2$As have 108 atoms. The full structural relaxation of the bulk models were performed and the calculated structural lattice parameters of the bulk structures are given in Table 1. We found that the lattice constants were in agreement with the experimental data. These comparisons confirm that our computational parameters are reasonably satisfactory and the DFT was able to calculate the bulk structural properties.

Table 1. The relaxed lattice constants for PtAs$_2$, PtAsS and Pd$_2$As bulk structures.

Structure	Lattice parameters (Å)	
	Calculated	Experimental
PtAs$_2$	a = b = c = 6.061	a = b = c = 5.970 [15]
PtAsS	a = b = c = 6.024	a = b = c = 5.790 [13]
Pd$_2$As	a = b = 6.737, c = 3.664	a = b = 6.620, c = 3.600 [16]

(a)   (b)   (c)
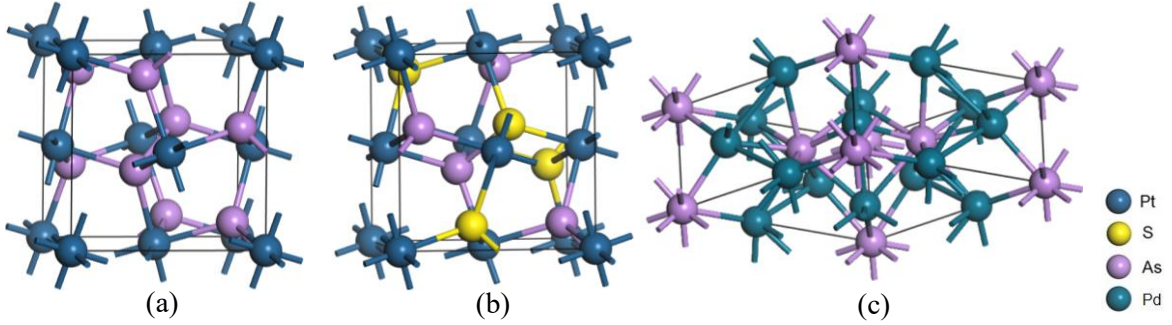
Figure 2: The relaxed bulk structure: (a) Sperrylite (PtAs$_2$), (b) platarsite (PtAsS) and (c) palladoarsenide (Pd$_2$As).

3.3. Vibrational properties of PtAs$_2$, PtAsS and Pd$_2$As

The analysis of vibrational properties of PtAs$_2$, PtAsS and Pd$_2$As phases with respect to the phonon dispersion are shown in Figure 3. The vibrational stability of the structures PtAs$_2$, PtAsS and Pd$_2$As were carried out along the symmetry directions within the first Brillouin zones.
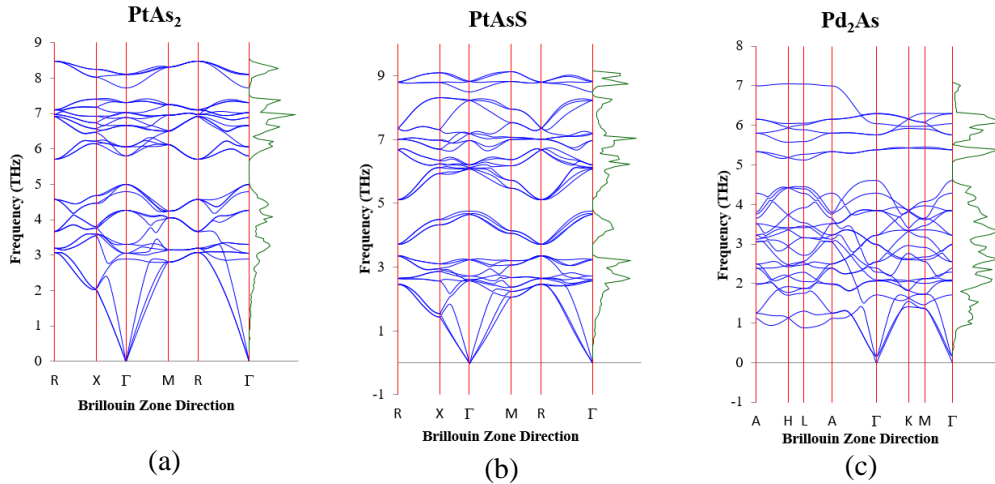

(a)   (b)   (c)

Figure 3: The phonon dispersion curves: (a) PtAs$_2$, (b) PtAsS and (c) Pd$_2$As structures.

We observed positive frequencies in all the Brillouin zone directions. As such, our phonon dispersion calculations confirm that PtAs$_2$, PtAsS and Pd$_2$As structures are vibrationally stable due to the absence of negative vibrations (soft modes).

3.4. Surface terminations and slab convergence

Considerations must be given to the large number of the Miller index planes (MI), and within each plane, all possible bulk terminations that exist. To reduce the search for working surfaces to a computationally tractable problem, whilst also ensuring that the most likely surfaces were surveyed, only the bulk terminations on the three low MI planes (100), (110) and (111) that are less reactive were considered. The desired surface terminations were precisely cleaved considering all possible terminations that are less reactive.
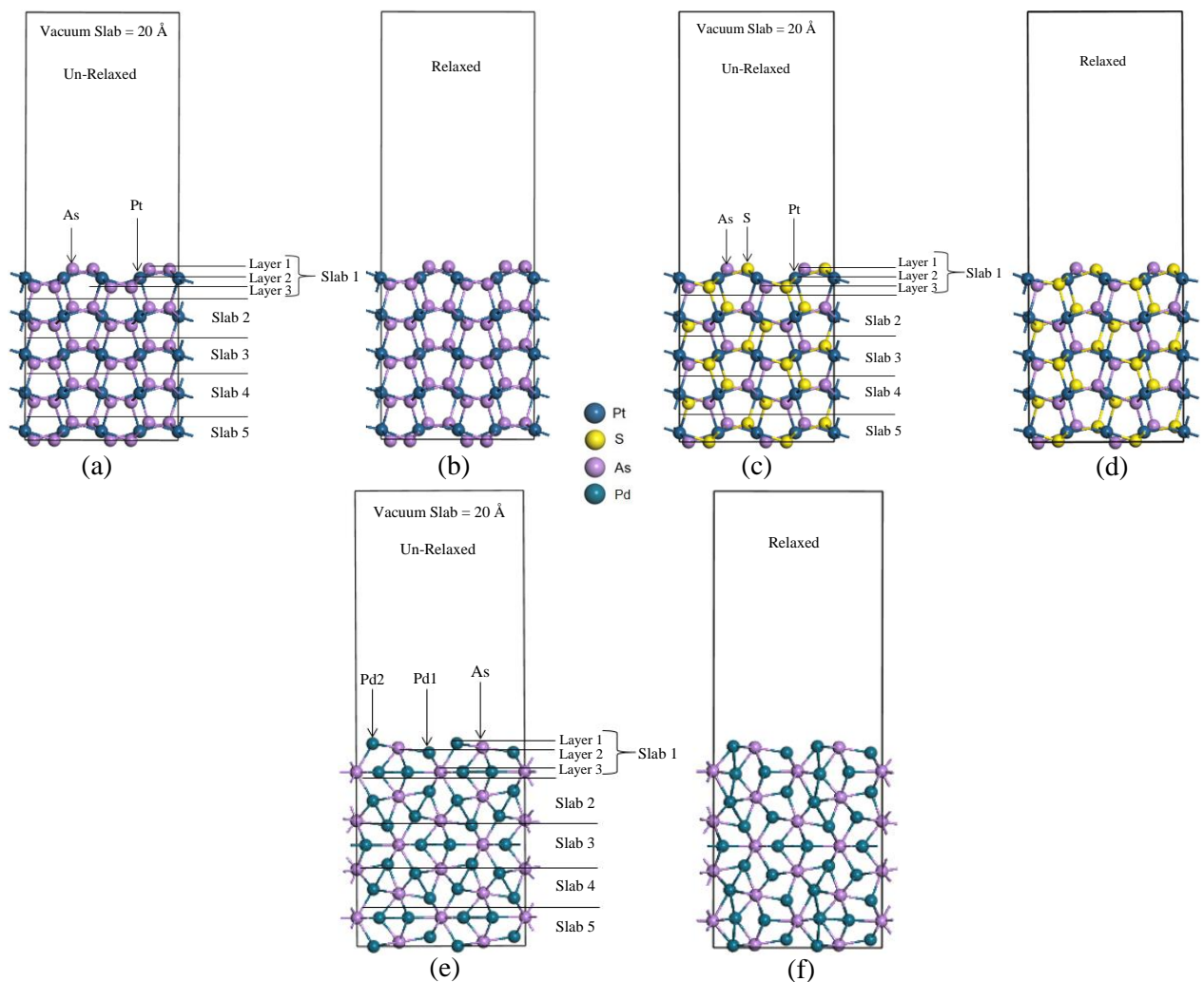

Figure 4: The un-relaxed and relaxed supercell structures of surface layers convergence for (a) and (b) PtAs$_2$, (c) and (d) PtAsS and (e) and (f) Pd$_2$As (100) surface.

The slab depth was varied and the 15-layer slab depth was chosen and considered as thick enough for adsorption. It was used to create a 2x2 supercell structures, which was then optimized allowing only the atom position to relax. Figure 4 shows the un-relaxed and relaxed supercell structures for (100) surface of PtAs$_2$, PtAsS and Pd$_2$As structures. Figure 4(e) showed the slabs that are not identical due to the stacking configuration [3]. The surface stabilities for different terminations were determined from the surface energies using equation 1:

$$E_{surface} = \left(\frac{1}{2A}\right)\left[E_{slab} - (n_{slab})(E_{bulk})\right] \tag{1}$$

where E_{slab} is the total energy of the cell containing the surface slab, n_{slab} is the number of atoms in the slab, E_{bulk} is the total energy per atom of the bulk and A is the surface area. A low positive value of $E_{surface}$ indicates stability of the surface termination [3].

Table 2 shows the supercell surface energies after relaxation for $PtAs_2$, PtAsS and Pd_2AS structures. The computed surface energies increase as: (100) < (111) < (110) for $PtAs_2$ and PtAsS and as (100) < (110) < (111) for Pd_2As. The (100) surface was identified as the most stable surface (working surface) since it displayed the lowest positive energies. Similar working surface for $PtAs_2$ was reported by Waterson et al. [3].

Table 2. The relaxed surface energies for $PtAs_2$ PtAsS and Pd_2As structures.

Surface slab	Surface energy (eV/Å^2)		
	$PtAs_2$	PtAsS	Pd_2As
100	0.065	0.035	0.070
111	0.085	0.062	0.109
110	0.091	0.717	0.097

3.5. Surface morphologies

The crystal morphology of $PtAs_2$, PtAsS and Pd_2As structures were predicted by using calculated surface energies of (100), (110) and (111) surfaces as shown in Table 2 using the METADISE code [17]. The calculated thermodynamical equilibrium morphologies of the relaxed (100), (110) and (111) surfaces are shown in Figure 5. Our surface morphologies results indicated that (100) surface was the most dominant surface exposed, followed by (111) and (110) surface for $PtAs_2$ model, with the (110) plane being the smallest. For PtAsS, the surface morphology showed that the mineral preferred to cleave only along the (100) surface plane, since the (110) and (111) surface plane did not appear on the morphology. Furthermore, the (100) surface was the dominant surface exposed on surface morphologies for Pd_2As model. However, in this case the (110) and (111) were also exposed largely, suggesting that these planes may cleave during mineral crushing.
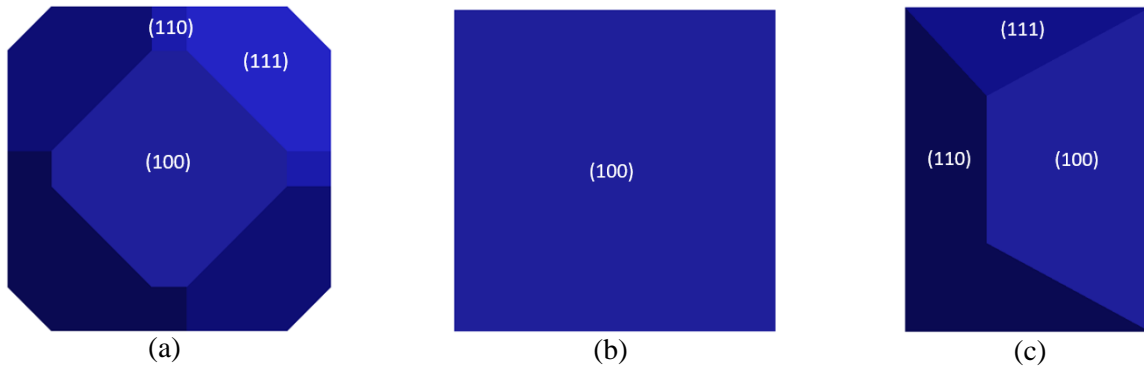

(a)   (b)   (c)

Figure 5: The calculated equilibrium morphologies. (a) $PtAs_2$, (b) PtAsS, and (c) Pd_2As surface structures.

4. Conclusion

In this study, we have performed *ab-initio* DFT calculations to investigate the bulk structural, vibrational and surface properties of $PtAs_2$, PtAsS and Pd_2As minerals. The optimized bulk structural lattice parameters were in agreement with the available experimental values. The phonon dispersion curves showed no soft modes along high symmetry direction suggesting stability for all structures. The PtAsS cluster expansion generated structures were found thermodynamically stable, with the 50:50 (x = 0.5) being the most stable phase. The calculated surface energies indicated that the (100) surface for $PtAs_2$, PtAsS and Pd_2As structures was the most stable amongst the low Miller index (100), (110) and (111).

Thermodynamical equilibrium morphologies of the relaxed structures indicated that (100) surface was the most dominant surface. These findings gave more insights on the bulk and surface stability of these minerals which demonstrated the preferred plane cleavage of these minerals that may be applicable in their recovery.

Acknowledgements

References

[1] Schouwstra R P, Kinloch E D and Lee C A 2000 Platinum excavation on the UG-2 reef in South Africa *Platinum Met. Rev.* **44** 33–39

[2] Viljoen M J and Schurmann L W 1998 Platinum-group metals *Miner. Resources. S. Afr.* **23** 532–568

[3] Waterson C N, Tasker P A and Morrison C A 2015 Design, synthesis and testing of reagents for high-value mineral collection, Edinburgh: The University of Edinburgh

[4] Manassidis I, De Vita A and Gillan M J 1993 Structure of the (0001) surface of Al_2O_3 from first principles calculations *Surf. Sci. Lett.* **285** 517–521

[5] Hohenberg P and Kohn W 1965 Inhomogeneous electron gas *Phys. Rev.* **136** 864–871

[6] Perdew J, Burke K and Ernzerhof M 1996 Generalized gradient approximation made simple *Phys. Rev. Lett.* **77** 3865–3868

[7] Kresse G and Furthmüller J 1996 Efficient iterative schemes for ab-initio total-energy calculations using a plane-wave basis set *Phys. Rev. B.* **54** 11169–11186

[8] Monkhorst H F and Pack J D 1976 Special points for Brillouin-zone integrations *Phys. Rev. B.* **13** 5188–5192

[9] Parlinski K, Li Z Q and Kawazoe Y 1997 First-principles determination of the soft mode in cubic ZrO_2 *Phys. Rev. Lett.* **78** 4063–4066

[10] Lee R and Raich J 1972 Cluster expansion for solid orthohydrogen *Phys. Rev. B.* **5** 1591–1604

[11] Sanchez J M, Ducastelle F and Gratias D 1984 Generalized cluster description of multicomponent systems *Physica A: Stat. Mech. Appl.* **128** 334–350

[12] Lerch D, Wieckhorst O, Hart G L W, Forcade R W and Muller S 2009 UNCLE: a code for constructing cluster expansions for arbitrary lattices with minimal user-input *Modelling Simul. Mater. Sci. Eng.* **17** 1–19

[13] Cabri L J, Laflamme J H G and Stewart J M 1977 Platinum group minerals from the onverwacht *Can. Mineral.* **15** 385–388

[14] Cabri L J, Laflamme J H G, Stewart J M, Rowland J F and Chen T T 1975 New data on some palladium arsenides and antimonides *Can. Mineral.* **13** 321–335

[15] Ngoepe P E, Ntoahae P S, Mangwenjane S S, Sithole H M, Parker S C, Wright K V and de Leeuw N H 2005 Atomistic simulation studies of iron sulphide, platinum antimonide and platinum arsenide *J. Sci.* **101** 480–483

[16] Olowolafe J O, Ho P S, Hovel H J, Lewis J E and Woodall J M 1979 Contact reactions in Pd/GaAs junctions *J. Appl. Phys.* **50** 955–962

[17] Watson G W, Kesley E T, de Leeuw N H, Harris D J and Parker S C 1996 Atomistic simulation of dislocations, surfaces and interfaces in MgO *J. Chem. Soc. Faraday. Trans.* **92** 433–438